

Hydrophobic/hydrophilic surface modification within buried air channels

Jose Luis Salas-Vernis, Joseph Paul Jayachandran, Seongho Park, Hollie A. Kelleher, Sue Ann Bidstrup Allen, and Paul A. Kohl^{a)}

School of Chemical and Biomolecular Engineering, Georgia Institute of Technology, Atlanta, Georgia 30332-0100

(Received 1 October 2003; accepted 1 March 2004; published 26 April 2004)

Recently, a method for fabricating air channels using a photodefinable sacrificial material (Unity 2203P) with acid-catalyzed degradation at low temperature was reported [J. P. Jayachandran *et al.* *J Microelectromech. Syst.* **12**, 147 (2003)]. The acid is created via a 'photoacid' generator (PAG) either photolytically (when exposed to UV irradiation) or thermolytically (when heated to the decomposition temperature of the PAG). This approach to the fabrication of micro air-channel structures using low-temperature decomposable sacrificial materials has applications to air-gap formation for electrical/optical interconnects, microelectromechanical systems, microfluidics, and microreactors. In this study, the surface characteristics of the silica surface after the decomposition of Unity 2203P was explored. It was found that the surface inside the air-channel after low-temperature Unity 2203P decomposition was hydrophilic and was then converted to hydrophobic after higher-temperature treatment. The modification of the silicon surface using silane-based chemistries and a method for creating alternating hydrophobic/hydrophilic textures within a buried air channel has been demonstrated. Trifluoropropyl dimethylchlorosilane was the most effective surface treatment for creating hydrophobic channels. The hydrophobic/hydrophilic nature of the silicon surfaces is shown by the contact angle measurements and x-ray photoelectron spectroscopy analyses. © 2004 American Vacuum Society. [DOI: 10.1116/1.1715084]

I. INTRODUCTION

Microfluidic devices using buried air channels offer a wide range of potential applications in the areas of sensors, separations, and combinatorial analysis.¹⁻⁴ One of the critical functions necessary for reproducible operation is the fabrication of reliable pumping devices. Pumping devices, which can deliver metered (i.e., drop wise) amounts, are especially important for analytical microfluidic devices. For example, Handique *et al.*⁵ have presented a nanoliter pumping scheme based on alternating hydrophobic/hydrophilic regions within the fluidic channel. The control of the hydrophilic/hydrophobic nature of the inside lining of microfluidic channels is important for wetting and mixing properties. In addition, it is highly desirable for the air channels used in microelectronic devices, such as for air insulation around electronic interconnects, to have a hydrophobic nature.⁶ Adsorbed moisture can lead to a high dielectric constant and corrosion.

Recently, a method for fabricating buried channels on silicon and other substrates using photosensitive sacrificial polymers has been demonstrated.¹ This processing method uses photodefinable polycarbonate-based formulations (Unity 2203P, Promerus LLC) for the fabrication of air gaps. The photosensitive polymer lowers the decomposition temperature of the sacrificial material. The ability to directly photopattern the air-channel regions reduces the number of processing steps compared to nonphotosensitive formulations. Polycarbonates are known to thermally decompose at low temperatures (200 °C to 350 °C). The addition of a catalytic

amount of a photoacid generator (PAG), such as diphenyl iodonium salts or triphenyl sulphonium salts, to the polycarbonate makes the polymer film (after spincoating) photosensitive. Upon exposure to UV irradiation or by sufficient thermal heating, the PAG reacts to produce a strong acid. The resulting acid catalyses the decomposition of the polycarbonate by cleaving the labile carbonate linkage of the polymer.¹ The acid adds to the carbonyl group of the carbonate destabilizing the polymer backbone and allowing a lower-temperature decomposition. A typical fabrication process using Unity 2303P involves six steps, as shown in Fig. 1: (1) Unity 2303P was spincoated onto a substrate, (2) the wafer was soft baked on a hotplate at 110 °C to 120 °C for 10 min, (3) the polymer was exposed to UV irradiation ($\lambda = 248$ nm) at 1 J/cm², (4) the film was baked at 110 °C to 120 °C for 1 to 10 min to decompose the exposed polymer, resulting in the definition of the air-channel regions, (5) the remaining sacrificial polymer was encapsulated by a overcoat material, such as a polymer or SiO₂; and (6) the encapsulated sacrificial polymer was decomposed by heating at 180 °C to form air gaps in the encapsulated regions.

In this article, the hydrophobic/hydrophilic nature of the surfaces after Unity 2203P decomposition is reported. The surface properties are shown to depend upon the temperature and atmosphere during decomposition, and the residual residue from decomposition. Surface modifications via silane-based reactions are shown to be effective in reversing the hydrophobicity of the surfaces. Lastly, a processing scheme for creating alternating hydrophobic/hydrophilic regions within a buried air channel is demonstrated.

^{a)}Electronic mail: paul.kohl@che.gatech.edu

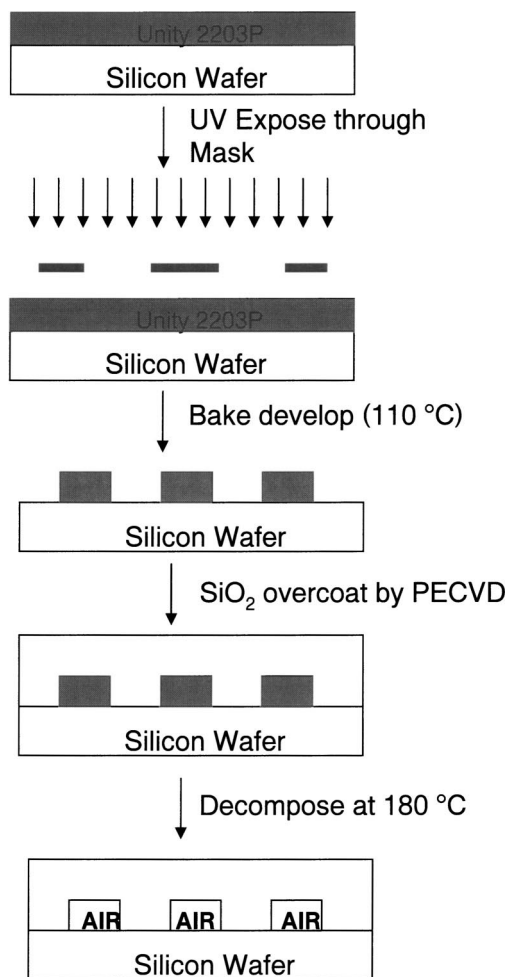


FIG. 1. Process of fabrication of air channels using Unity 2203P.

II. EXPERIMENT

Unity 2203P (Promerus LLC, Brecksville, OH) was spincoated onto silicon wafers and photopatterned as previously described.¹ Decomposition of the exposed Unity 2203P was carried out at 110 °C to 120 °C producing gaseous (i.e., dry) products. Decomposition of the unexposed Unity 2203P occurs at ~180 °C at the Lindberg furnace in a nitrogen atmosphere. Exposed and unexposed regions on the same wafer were fabricated by the use of standard lithographic masks and exposure tools. The samples were heated in the nitrogen-purged tube oven or on a hotplate with ambient air.

The surface hydrophilicity or hydrophobicity was determined by measuring the contact angle using a water drop and video contact angle 2500XE system (AST products). The contact angle measurements were repeated many times across each sample and the (\pm) reported values represent the 95% confidence interval.

The silicon samples were first exposed to HNO₃ vapors at an ambient temperature for 10 min prior to silane treatment to acidify the surface, unless otherwise noted. The silane treatments were carried out on a vacuum line. A turbomolecular pump was used to evacuate the silicon samples. The silane-based compounds were loaded into a separate vessel

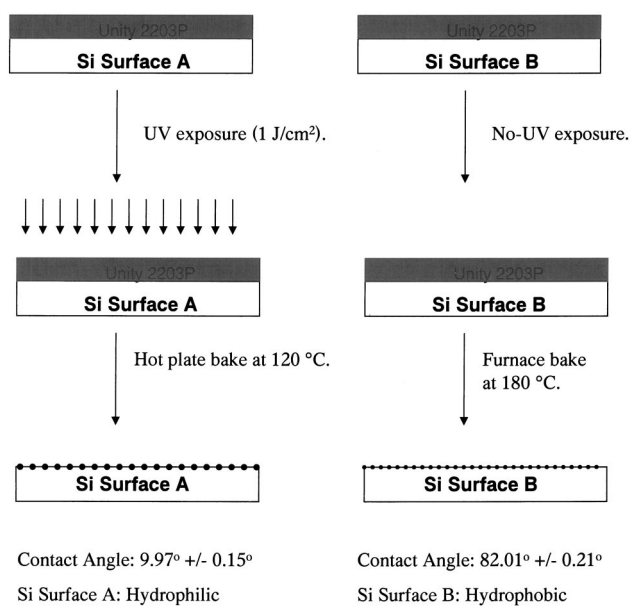


FIG. 2. Process for fabrication of hydrophilic and hydrophobic surfaces.

under nitrogen. The nitrogen gas was evacuated so that only the silane gas existed in the head space. The silicon samples were exposed to the silane vapors during treatment.

The elemental composition of the residual material remaining after decomposition of the sacrificial polymers on the surface was determined by x-ray photoelectron spectroscopy (XPS). XPS measurements were carried out with a Physical Electronics model 1600 XPS system using an aluminum $K\alpha$ source and toroidal monochromator. All analyses were setup with a 0.8 mm spot size and 45° take-off angle. The base pressure was less than 5E-9 Torr. Ar-ion sputtering was used for depth profiling of the surface composition. The Ar-ion sputtering rate was 3 nm/min for SiO₂. It was assumed that the rate was the same for the surface films.

III. RESULTS AND DISCUSSIONS

A. Surface properties of Unity 2203P

The nature of the surface residue from Unity 2203P decomposition was characterized. Figure 2 shows the process sequence for the fabrication of hydrophilic and hydrophobic surfaces. The Unity 2203P was spincoated to a thickness of 1 μ m on a thermally oxidized silicon wafer. One-half of the wafer was exposed to 248 nm light at a dose of 1 J/cm². The wafer was heated in a nitrogen-purged tube furnace at 120 °C for 2 h. The treatment at 120 °C activated the PAG in the Unity 2203P, which catalyzes the decomposition of the polymer. Thus, the Unity 2203P, which was exposed to UV light, decomposed while the unexposed regions remained at full thickness. The contact angle of a water drop on the surface was measured on each region on the wafer. In the exposed region where the Unity 2203P decomposed, the contact angle was 9.97° \pm 0.15°. A low contact angle, such as this, represents a hydrophilic surface where the water drop spreads out across the silicon surface. The low contact angle

TABLE I. Contact angle measurements used for the evaluation of hydrophobic coupling agents. The errors displayed were evaluated at the 95% confidence interval.

	TMMS	PDMES	TFS
Contact angle before TFS treatment	29.83 ± 3.06	33.23 ± 1.53	31.28 ± 0.62
Contact angle after TFS treatment	67.63 ± 3.12	67.73 ± 1.37	82.91 ± 3.00

is due to the presence of polar volatiles, which remain after the photolytic decomposition of the Unity 2203P. In the unexposed regions where the Unity 2203P was not decomposed, the contact angle was $82.95^\circ \pm 0.15$. A similar hydrophobic surface was observed for Unity 2203P after spincoating (i.e., polymer surface where no decomposition occurred).

A second Unity 2203P sample on silicon was prepared and decomposed at 180°C after one-half of the wafer was exposed to UV irradiation. In this case, the Unity 2203P on both sides of the wafer decomposed since the temperature was above the thermal decomposition temperature of the PAG. Thus, acid was generated in the non-UV irradiated region via thermal means. The contact angle in the region exposed to UV light was $85.38^\circ \pm 0.15^\circ$ and the contact angle in the non-UV-exposed region was $82.01^\circ \pm 0.21^\circ$. Thus, both portions of the wafer heated to 180°C were hydrophobic with little difference in surface behavior due to irradiation. Only the 120°C decomposition under UV exposure resulted in a hydrophilic surface.

B. Surface modification of surface silanols of silica using silane-based compounds

In order to change the hydrophobicity of the surface after Unity 2203P decomposition, several silane-based surface modification compounds were investigated. Silanes are commonly used as coupling agents in a variety of areas ranging from microelectronics to construction and aerospace composites.^{7,8} The creation of covalently bonded silicon-coupled layers on the surface using silane-based compounds is well documented in literature.^{9–11}

The contact angle of a water drop on the surface of the wafer was measured before and after each silane treatment. Table I shows the contact angle results for vapor treatment with trimethyl methoxysilane (TMMS), phenyldimethyl ethoxysilane (PDMES), and trifluoropropyl dimethylchlorosilane (TFS). The structures of TMMS, PDMES, and TFS and the reactions between the silanol surface groups are depicted in Figs. 3 and 4, respectively. The TFS treatment resulted in the most hydrophobic surface (i.e., highest contact angle, $82.91^\circ \pm 3.00^\circ$). Thus, TFS was used in the experiments to modify the surfaces and produce an alternating hydrophobic/hydrophilic surface.

First, the chlorosilane or alkoxy silane group can be hydrolyzed to produce silanol and liberate the corresponding alcohols (methanol and ethanol when TMMS and PDMES is used, respectively) or to produce HCl. In the second step, the

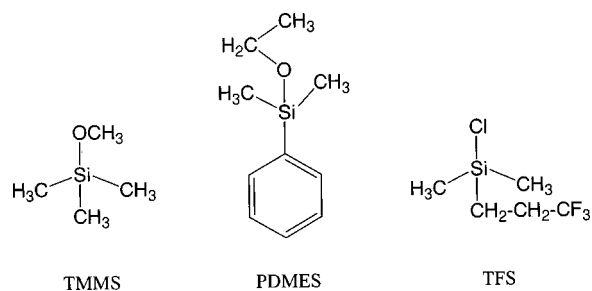


FIG. 3. Silane-based compounds used surface modification in the present study.

silanol from the silane-based compounds undergoes a condensation reaction with the surface silanol groups (—OH) to form a monolayer surface coverage. The surface coverage converts the surface from hydrophilic to hydrophobic. Alternatively, the Si—Cl group of TFS can react with the surface silanol group (—OH) to form Si—O—Si bonds and HCl. A similar reaction is reported¹⁰ when 1H, 1H, 2H, 2H-perfluorodecyltri-chlorosilane is used as a silane-coupling agent. In our experiments, TFS gave a surface with a high contact angle ($82.91^\circ \pm 3.00$) and, therefore, more hydrophobic than TMMS ($67.63^\circ \pm 3.12$) and PDMES ($67.73^\circ \pm 1.37$).

The presence of the trifluoromethane group in TFS on the silicon surface causes the repulsion of water and makes the surface more hydrophobic compared to the methyl and phenyl

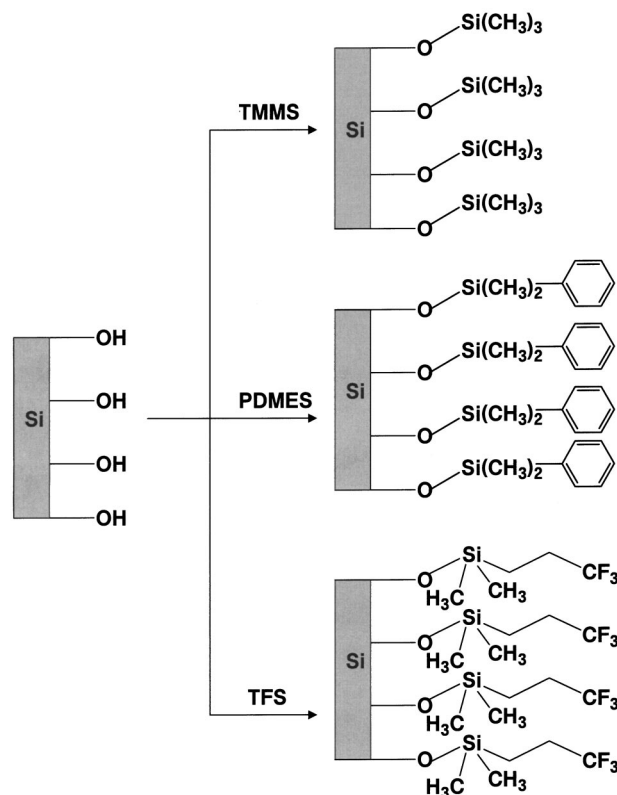


FIG. 4. Reaction between gaseous TMMS, PDMES, and TFS and the surface silanol groups on silica.

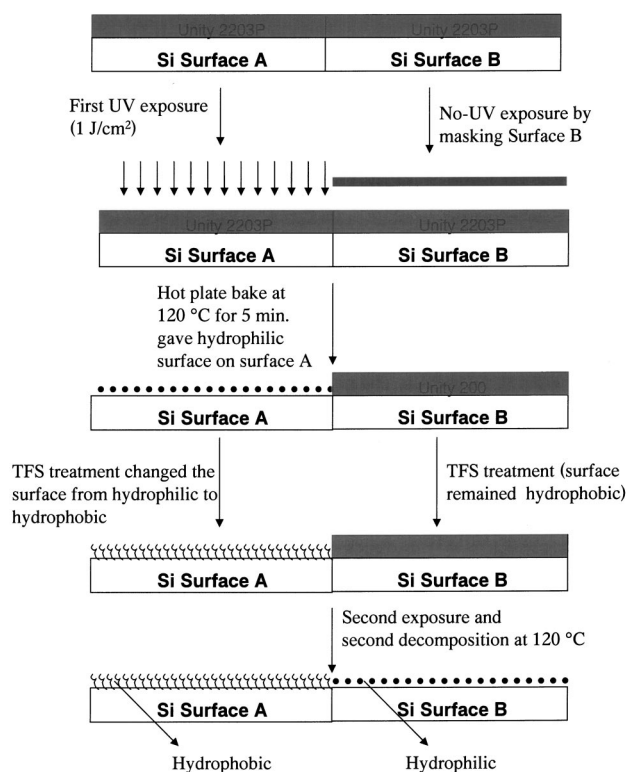


FIG. 5. Process for fabrication of hydrophilic and hydrophobic surfaces.

nyl groups in TMMS and PDMES, respectively. Also, the reaction could be faster due to the presence of trifluoromethane group. This may be attributed to the fact that the highly electronegative fluorine groups withdraw electron density from the silicon leaving it highly electrophilic and reactive with the surface silanol. It may also be postulated that the TFS can be easily hydrolyzed under the atmospheric humidity. A similar mechanism was proposed⁹ when *n*-octadecyltrichlorosilane was used as a silane-based compound and reacted to the silanol group of silica. Only monolayer coverage is expected for each surface treatment compound because the silanes were monofunctional and not capable of multilayers.

C. Mixed hydrophobic/hydrophilic surface

The TFS treatment experiments were used to fabricate alternating hydrophobic/hydrophilic surfaces. A variety of exposure times were used ranging from 0.17 min. to 2 h. The contact angle of Unity 2203P films exposed to TFS (before and after decomposition, with and without UV exposure) was measured. Figure 5 shows the process sequence for the fabrication hydrophilic/hydrophobic surface on a silicon wafer. The surface that is decomposed after the TFS treatment is not as hydrophilic as the surface that is decomposed before the TFS treatment (9.75° versus 42°). A 4 in. silicon wafer was coated with Unity 2203P, soft baked at 120 °C. The thickness of the film was approximately 1.5 μm. The wafer was then cleaved into small rectangular pieces (2 in. length and 0.5 in. width). One-half of each wafer strip was exposed

TABLE II. Contact angle measurements after the second exposure and second decomposition at 120 °C for various TFS treatment times. All reactions were carried out at 100 °C. The errors displayed were evaluated at the 95% confidence interval.

Time (min)	Contact angle (°)	
	Surface A	Surface B
120	92.43 ± 10.48	82.50 ± 1.18
5	97.25 ± 2.96	47.29 ± 2.49
1	94.48 ± 2.80	42.55 ± 2.51
0.5	98.23 ± 2.34	46.44 ± 1.37
0.17	95.34 ± 3.08	56.29 ± 5.71
Control	9.57 ± 0.57	76.57 ± 1.29

to UV light at 1 J/cm². The wafers were then heated on a hotplate at 120 °C resulting in the decomposition of the UV exposed Unity 2203P. This produces two surfaces, surface A (UV exposed and decomposed at 120 °C) and surface B (no UV exposure leaving the polymer film in place on the surface).

Contact angle experiments showed surfaces A and B to be hydrophilic and hydrophobic, respectively. (Note, surface A is the silicon surface and surface B is the polymer surface.) The sample was then treated with TFS at 100 °C for 2 h under a vacuum. The previously hydrophilic surface (surface A) was modified and converted to hydrophobic due to the TFS reaction. The second UV exposure (1 J/cm²) and a second heating at 120 °C changed the previously hydrophobic surface B to hydrophilic. The second heating resulted in decomposition of the Unity 2203P in the region not previously decomposed during the first heating. Table II shows the contact angle for both sides of the wafer surface A (UV exposed with decomposition at 120 °C and after TFS treatment at 100 °C), and surface B (decomposition after TFS treatment). The contact angle experiment on a control sample (that is, before the TFS treatment) showed a lower contact angle due to the hydrophilic nature of the surface.

The results show that the TFS treatment converted the hydrophilic surface to hydrophobic, as seen before. It is also noted that surface B (decomposed after TFS treatment), was found to be hydrophobic because the sacrificial polymer covered the surface during TFS treatment blocking it from the silane reaction. The only exception to the hydrophilic surface (surface B) after the second UV exposure and second decomposition was when the TFS treatment was performed for 120 min. In this case, instead of producing a hydrophilic surface, it gave a hydrophobic surface (contact angle being 82.50 ± 1.18). It appears that the TFS treatment (for 120 min and at reaction temperature, 100 °C) loads the Unity 2203P to such an extent that the surface after decomposition had a hydrophobic character.

A duplicate set of experiments was performed with shorter TFS reaction times and at lower reaction temperature (25 °C). The results shown in Table III show a similar trend in contact angle as observed in Table II. Thus, it is possible to convert the hydrophilic surface resulting after UV exposure and 120 °C heating from hydrophilic to hydropho-

TABLE III. Contact angle measurements after the second exposure and second decomposition at 120 °C for various TFS treatment times. All reactions were carried out at 25 °C. The errors displayed were evaluated at the 95% confidence interval.

Time (min)	Contact angle (°)	
	Surface A	Surface B
30	83.15 ± 3.24	39.28 ± 4.77
10	85.08 ± 1.79	41.05 ± 2.41
5	83.23 ± 4.36	39.58 ± 2.11
1	89.11 ± 3.18	38.93 ± 3.82

bic without disturbing the unexposed regions by controlling the TFS treatment time and at room temperature (25 °C).

It was also found in separate experiments (temperature being the variable) that a TFS exposure as short as 5 min at 25 °C was effective in converting the surface from hydrophilic to hydrophobic. Figure 6 shows the results of contact angle measurements for two wafers coating with Unity 2203P to thickness of 1 μm and 5 μm. As described above (Fig. 5), one-half of each wafer was exposed UV irradiation at 1 J/cm², heated to 120 °C for 2 h (resulting in decomposition of the Unity 2203P in the exposed regions). The contact angle of the decomposed regions showed a hydrophilic surface. After TFS treatment at 25 °C for 5 min, the decomposed side had a similar contact angle as the unexposed side (i.e., hydrophobic). The full wafer was then exposed to UV irradiation and heat treated a second time at 120 °C. It should be noted that the regions, which had been decomposed during the first heating and exposed to TFS, retained their hydrophobic nature. The regions, which were decomposed on the second heating step after TFS exposure, converted to a hydrophilic surface, as demonstrated above. Thus, only a short TFS treatment was necessary. In addition, the film thickness of the Unity 2203P (i.e., 1 μm versus 5 μm) did not have an effect on the results.

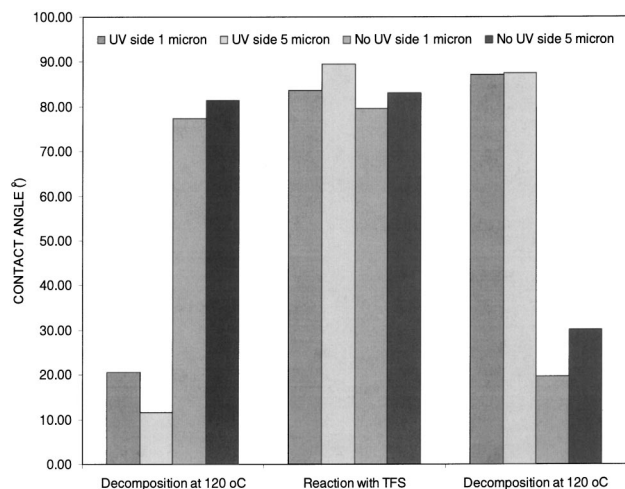


FIG. 6. Contact angle of the silicon wafer after the first decomposition of PPC at 120 °C, after the reaction with TFS for 2 min at 25 °C, and after the second decomposition at 120 °C.

D. Residue analysis using x-ray photoelectron spectroscopy

XPS was used to determine the elemental composition of residual material remaining after decomposition of the sacrificial polymers on sputtered Au films. Unity 2203P was spin-coated onto two different 4 in. Ti/Au-coated silicon wafers, then soft baked at 110 °C for 10 min. The thickness after soft baking was 1.5 μm and 5.4 μm. Each sample was divided into two pieces. One piece of each thickness was blanket exposed at 1 J/cm² (as before). Following exposure, the photoactivated samples were decomposed by baking on a hot-plate at 110 °C for 3.5 min (sample names: 1.5 μm-Photo PAG & 5.4 μm-Photo PAG). The unexposed samples were thermally decomposed in a nitrogen-purged Lindberg tube furnace ramped at 10 °C/min to 180 °C and held for a period of 3 h (sample names: 1.5 μm-Thermal PAG & 5.4 μm-Thermal PAG). XPS was used to analyze the elemental composition of the surface residues. The analysis was also performed after 20, 40, and 170 s of Ar sputtering. The atomic percentage of all elements detected was then determined from the area under each peak, with an accuracy of approximately ± 1%.

The XPS results are shown in Table IV. The residues consist of a combination of the elements C, O, F, and I. Au was also observed when the x-ray analysis depth reached the metal film below the residue material. Table IV shows analysis for decomposition of two thicknesses (1.5 μm and 5.4 μm) and two PAG decomposition mechanisms [thermal and photo (UV) exposure].

Oxygen was detected in a substantial concentration only on the surface of the residual films and therefore was thought to be a result of environmental contamination. A small percentage of oxygen was detected throughout the sample, 5.4 μm-Thermal PAG and is likely from the Unity 2203P. Figure 7 shows the C 1s XPS spectrum for sample 1.5 μm thick Unity 2203P decomposed by thermal activation of the PAG. This spectrum is typical of all four samples and shows two distinct C 1s peaks. The peak at a binding energy of 284 eV is typical to C—C, C—H, and C=C carbons. A second peak is seen around 287 eV, which indicates the presence of C—O or C—OH groups. Following a brief 20 s sputter, the C—O, C—OH peak disappears. The scans taken after all subsequent sputters show only the single peak at 284 eV. The oxygen and C—O carbon seen on the top surface is accounted for from atmospheric contamination, such as CO₂ absorption to the surface. A small amount of iodine was detected in the samples decomposed through the photolytic-induced acid-catalyzed reaction, but not in the thermal-induced acid-catalyzed reaction. This is because of the lower-temperature (110 °C) decomposition performed when the samples were UV irradiated. When the sample was not UV irradiated, the decomposition was performed at 180 °C for 2 h. One of the detected volatiles from the decomposition of the PAG is iodobenzene which has a high boiling point (188 °C/760 mm Hg). That is why the trace of this volatile (iodobenzene) that was present in the residue from the photo-induced catalyzed reaction sample was not present when the

TABLE IV. XPS results of the elemental composition of residual material remaining after decomposition of the sacrificial polymers. The analysis was performed on the exposed surface and after Ar-ion sputter etching. The depth of Ar-ion sputter etching corresponds to the rate measured for SiO₂ etching.

Sample	Elements detected	Atomic percentage				
		C	O	F	I	Au
1.5 μm-Photo PAG						
Surface scan	C, O, F, I	64.2	2.8	32.8	0.26	N/D
1 nm Ar sputter	C, F, I, Au	82.2	N/D	16.5	0.31	0.99
2 nm Ar sputter	C, F, I, Au	88.3	N/D	10.4	0.15	1.2
9 nm Ar sputter	C, F, Au	90.2	N/D	7.1	N/D	2.7
5.4 μm-Photo PAG						
Surface scan	C, O, F, I, Au	67.8	1.9	30.0	0.26	0.03
1 nm Ar sputter	C, F, I, Au	79.8	N/D	19.9	0.21	0.12
2 nm Ar sputter	C, F, I, Au	84.5	N/D	15.2	0.21	0.13
9 nm Ar sputter	C, F, I, Au	91.4	N/D	8.3	0.19	0.14
1.5 μm-Thermal PAG						
Surface scan	C, O, F	66.4	10.3	23.2	N/D	N/D
1 nm Ar sputter	C, F	94.9	N/D	5.1	N/D	N/D
2 nm Ar sputter	C, F, Au	94.4	N/D	3.8	N/D	1.8
9 nm Ar sputter	C, F, Au	80.8	N/D	7.5	N/D	11.8
5.4 μm-Thermal PAG						
Surface scan	C, O, F	65.8	10.7	23.5	N/D	N/D
1 nm Ar sputter	C, O, F, Au	91.7	1.6	6.6	N/D	0.09
2 nm Ar sputter	C, O, F, Au	95.5	0.90	3.6	N/D	0.04
9 nm Ar sputter	C, O, F, Au	95.3	1.4	3.3	N/D	0.08

N/D: Not detected by XPS.

decomposition occurred without UV irradiation but was decomposed at a higher temperature (180 °C) for 2 h. In addition, Table IV shows that the percentage of fluorine present in the residues from photoinduced decomposition is higher.

The fluorine also originated from the PAG. This indicates that either (a) more PAG remains behind in the residue for the “photosamples” or (b) the carbon-based polymer undergoes a more complete decomposition when photolytically induced.

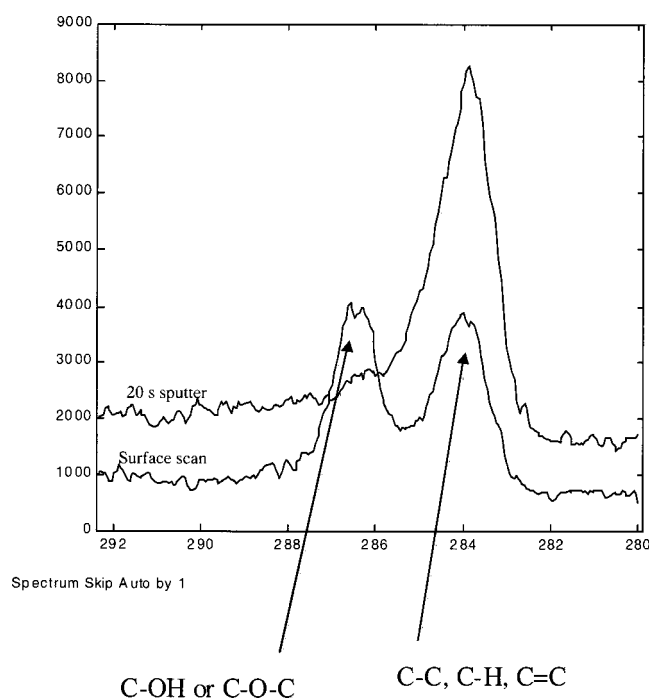


FIG. 7. Representative XPS spectrum of the residual elemental composition after the decomposition.

E. Residue thickness from atomic force microscopy

The thickness of the residue was analyzed by atomic force microscopy (AFM) using a Nanoscope IIIa AFM from Digital Instruments, Inc. This instrument was operated in contact mode using a flexible silicon cantilever to prevent the tip from breaking by sticking in crevices. The samples were prepared as in Table IV. Using a sharp edge, a portion of the film was removed from the substrate to form a step for thickness measurement. The initial polymer film thickness was measured using a Tencor P-15 contact Profilometer and the results are shown in Table V. Following decomposition, the AFM was used to measure the step height of the residual

TABLE V. Residual thickness measurement after decomposition by AFM.

Sample	Decomposition	Polymer film thickness (μm)	Residue thickness
Photo PAG	Hotplate, 110 °C, 3 min	1.6	41 ± 5 nm
Thermal PAG	Furnace, 180 °C, 2 h	1.55	28 ± 26 nm
Photo PAG	Hotplate, 110 °C, 3 min	6.21	73 ± 24 nm
Thermal PAG	Furnace, 180 °C, 2 h	6.15	54 ± 30 nm



Fig. 8. Example of an air channel fabricated using Unity2203P as a sacrificial polymer and $\sim 1 \mu\text{m}$ thick SiO_2 as an overcoat layer.

polymer film in the same location as the original thickness measurement. The results of these measurements are shown in the last column of Table V.

As seen in Table V, the thickness of the residual material increases slightly with original thickness. The XPS results demonstrate that the residual material contains a large percentage of fluorine, which comes from the PAG in the formulation. The PAG loading is based on the percent of dry polymer in the mixture. If all the residue was purely accounted for only by the PAG, the residual material would have a C:F ratio of approximately 2:1. However, the highest C:F ratio observed is about 4:1. Therefore, either some of the PAG anions are leaving the system, or additional C residue is present from the polymer. Comparing the $1.5 \mu\text{m}$ and $5.4 \mu\text{m}$ thick samples (both the thermal and photo samples), the relative percentages of C and F in the residues are approximately the same, though the final residue thickness varies.

Thinner residues result from the thermal-induced acid-catalyzed decomposition, than the photoinduced acid-catalyzed decomposition. In addition, the XPS results showed that the percentage of F remaining from photoinduced samples was higher than for the thermally-induced sample. The larger residue thickness is attributed to a higher amount of PAG being left behind in the film.

F. Alternating hydrophobic/hydrophilic regions in buried air channels

The experiments above have shown that hydrophobic and hydrophilic surfaces can be created side by side. Figure 1 shows the process sequence for fabricating buried air channels using Unity 2203P. Figure 8 shows an example of the fabricated air channel ($5 \mu\text{m}$ is the height) via the process sequence described in Fig. 1. The Unity 2203P was spin-coated to a thickness of $5 \mu\text{m}$ followed by patterning (UV exposure in regions to be decomposed followed by heating to 120°C). The remaining Unity 2203P was overcoated with plasma-enhanced chemical vapor deposited SiO_2 . The plasma deposition temperature was below the thermal de-

composition temperature of the polymer. A value of 150°C was used. Vent holes are not needed in the SiO_2 because the decomposition products permeate through the SiO_2 .^{1,2} The sample was UV irradiated at 1 J/cm^2 and heated to 120°C for 2 h. This caused the remaining Unity 2203P encapsulated in the SiO_2 to decompose creating a buried air cavity. The sample was then treated with TFS for 2 h at 25°C . Mechanical removal of the encapsulating SiO_2 showed that the exposed surface had a hydrophobic nature with a contact angle of 91° . When the air-gap regions were not exposed to TFS, the surface remained hydrophilic, as expected.

In a separate experiment, $100 \mu\text{m}$ wide Unity 2203P lines were fabricated, as described above, followed by SiO_2 encapsulation. A second lithography mask was used to expose alternating portions of the Unity 2203P (encapsulated in SiO_2) to UV irradiation. The sample was then heated to 120°C causing the irradiated regions to decompose. A single line was broken open and the contact angle in the decomposed region was 36° and the contact angle in the undecomposed Unity 2203P region (non-UV exposed region) was 98° . The remainder of the sample was treated with TFS for 30 min at 110°C and then UV exposed and heated to 120°C . This caused the remainder of the Unity 2203P (non-UV exposed region) to decompose. The original decomposition region, which had the TFS coating, had a contact angle of 85° and the decomposed region had a contact angle of 33° .

This shows that the TFS can penetrate the SiO_2 overcoat in the regions where an air gap exists, and the TFS can change the buried surface from hydrophilic to hydrophobic. Recall that the SiO_2 completely encapsulates the air channels so that the TFS has to permeate through the SiO_2 overcoat. These results are consistent with the previous experiments, but show that the surfaces can be decomposed side by side within a single air channel.

G. Surface analysis on the trifluoropropyl dimethylchlorosilane-treated microair channel

XPS surface analysis was performed to show the chemical changes of the air-gap surface due to TFS treatment. Unity 2203P was patterned followed by SiO_2 encapsulation. The sample was exposed to UV irradiation, as described above and the Unity 2203P was decomposed at 120°C to form air channels. Channels were cleaved from the array of fabricated channels on the silicon wafer. These channels were treated with TFS separately and analyzed for the presence of fluorine inside the channel and on the surface of the SiO_2 overcoat. XPS analysis was performed on the surfaces of the two samples with the SiO_2 encapsulation intact. The XPS analysis of the surface of the sample, with the SiO_2 in place, shows the presence of silicon, oxygen, and carbon, Figure 9 (scan a). Fluorine was not detected on the surface of the SiO_2 overcoat showing that the TFS did not react with the bare SiO_2 surface. The air channels were broken open and a second XPS analysis was performed on the surface inside the channel. As shown in Fig. 9 (scan b), fluorine was found in the interior of the TFS treated sample along with a higher

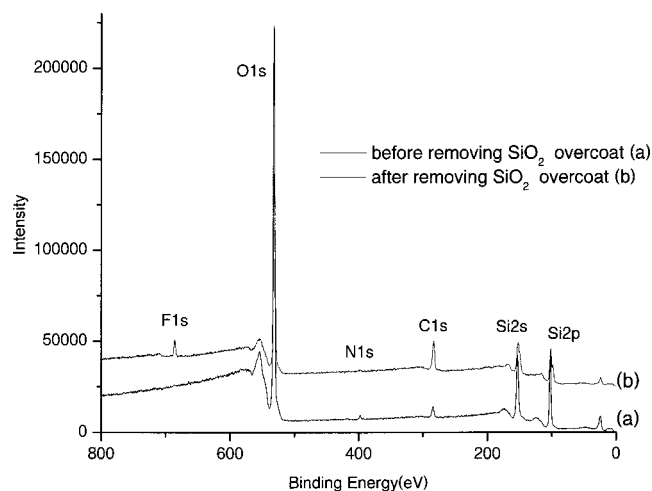


FIG. 9. XPS spectra of the samples performed on the surface of SiO_2 overcoat (scan a) and on the surface inside the channel after removing the SiO_2 overcoat (scan b).

carbon content, as compared to the channel top surface or buried channel not exposed to TFS. No fluorine was found in the interior of the air-channel sample, which were not exposed to TFS.

The XPS analysis is consistent with the conclusion that the TFS penetrates the SiO_2 overcoat, and reacts with the interior surface producing a hydrophobic surface. The fluorine from the trifluoropropyl group on the TFS was detected by XPS. Since TFS is a monofunctional silane (i.e., monochloro), once the TFS reacts with surface, the surface cannot react further (and build a thick layer of TFS). A single layer of TFS on the surface would be easily sputteretched. Each of these facts is consistent with the surface analysis and contact angle measurements.

IV. SUMMARY

The fabrication process of alternating hydrophilic/hydrophobic regions in microair channels is presented. The process involves the creation of hydrophilic microchannels

within an overcoat material (silicon dioxide) by the decomposition of a sacrificial polymer (Unity 2203P at 120°C) within an overcoat SiO_2 layer followed by the diffusion of 3,3,3 trifluoropropyl dimethyl chlorosilane (TFS), a hydrophobic coupling agent, through the overcoat material and the bonding of this coupling agent on the silicon surface. The most important parameter in the fabrication of hydrophobic channels involves the penetration of the silane through the overcoat material (SiO_2) and reaction with the surface. The silane reaction with the surface silanol groups was confirmed by contact angle measurements and XPS analysis studies. Thus, a process for producing alternating hydrophobic/hydrophilic regions within a buried air channel has been demonstrated.

ACKNOWLEDGMENTS

The technical discussions with and materials contribution from Promerus LLC, especially Dr. Edmund Elce and Dr. Robert Shick are gratefully acknowledged. The technical discussions with Professor Clifford Henderson, Professor Dennis Hess, and Christopher Timmons concerning contact angle studies, and XPS, respectively, are also gratefully acknowledged.

- ¹J. P. Jayachandran, H. A. Reed, H. Zhen, L. F. Rhodes, C. L. Henderson, S. A. Bidstrup-Allen, and P. A. Kohl, *J. Microelectromech. Syst.* **12**, 147 (2003).
- ²H. A. Reed, C. E. White, V. Rao, S. A. Bidstrup-Allen, C. L. Henderson, and P. A. Kohl, *J. Micromech. Microeng.* **11**, 733 (2001).
- ³H. A. Reed, M. S. Bakir, C. S. Patel, K. P. Martin, J. D. Meindl, and P. A. Kohl, *Proc. IEEE* 151 (2001).
- ⁴D. Bhusari, H. A. Reed, M. Wedlake, A. Padovani, S. A. Bidstrup-Allen, and P. A. Kohl, *J. Microelectromech. Syst.* **10**, 400 (2001).
- ⁵K. Handique, B. P. Gogoi, D. T. Burke, C. H. Mastrangelo, and M. A. Burns, *Proc. SPIE* **3224**, 185 (1997).
- ⁶J. D. Meindl, J. A. Davis, P. Zarkesh-Ha, C. Patel, K. Martin, and P. A. Kohl, *IBM J. Res. Dev.* **46**, 245 (2002).
- ⁷B. Arkles, *CHEMTECH* **7**, 766 (1977).
- ⁸E. Plueddemann, *Silane Coupling Agents* (Plenum, New York, 1991).
- ⁹D. F. Untereker, J. C. Lennox, L. M. Wier, P. R. Moses, and R. W. Murray, *J. Electroanal. Chem.* **81**, 309 (1977).
- ¹⁰J. Sajiv, *J. Am. Chem. Soc.* **102**, 92 (1980).
- ¹¹K. Handique, D. T. Burke, C. H. Mastrangelo, and M. A. Burns, *Anal. Chem.* **72**, 4100 (2000).